AIP | Review of Scientific Instruments

Optical fiber velocimetry: A technique for measuring velocity in two-dimensional flows

M. Rivera, A. Belmonte, W. I. Goldburg, X. L. Wu, and H. Kellay

Citation: Review of Scientific Instruments **69**, 3215 (1998); doi: 10.1063/1.1149086
View online: http://dx.doi.org/10.1063/1.1149086
View Table of Contents: http://scitation.aip.org/content/aip/journal/rsi/69/9?ver=pdfcov
Published by the AIP Publishing

Optical fiber velocimetry: A technique for measuring velocity in two-dimensional flows

M. Rivera,[a] A. Belmonte, W. I. Goldburg, and X. L. Wu[b]
Department of Physics and Astronomy, University of Pittsburgh, Pittsburgh, Pennsylvania 15260

H. Kellay
Centre de Physique Moleculaire Optique et Hertzienne, Universite Bordeaux I, 33405 Talence Cedex, France

(Received 5 May 1998; accepted for publication 14 June 1998)

In this article we describe a new technique, optical fiber velocimetry (OFV), to instantaneously measure two components of velocity at a point in freely suspended flowing liquid films. The technique relies on the measurement of displacements of an optical fiber tip which is coupled to the flowing film. The deflection of the fiber tip is proportional to the velocity and it behaves as a simple harmonic oscillator. Thus the low frequency response of the fiber gives direct measurements of the flow velocity. A statistical test using data acquired simultaneously by the fiber and by a laser Doppler velocimeter shows good agreement between the two techniques. Velocity power spectra measured in the wake of a von Karman street and in two-dimensional (2D) grid turbulence using the OFV also compare favorably with the laser Doppler velocimeter. The OFV technique is simple and robust, allowing it to be used in a wide variety of flows that have strong 2D characteristics. New prospects of using multiple fibers to measure circulation and velocity correlations at several separated spatial points are discussed. © *1998 American Institute of Physics.*
[S0034-6748(98)02109-1]

I. INTRODUCTION

Experimental fluid mechanics currently have three standard techniques for obtaining the time-resolved velocity field in a fluid.[1,2] Two of these, the hot-wire anemometer (HWA) and laser Doppler velocimeter (LDV), obtain velocity data at a single point in the flow with high bandwidth, typically in the kHz range. The third, particle imaging velocimetry (PIV), sacrifices temporal resolution, normally working at 30 Hz, for velocity information of whole fields of the flow. While these techniques are well established, they can cost tens of thousands of dollars to implement. In this article we present a new, simple, and inexpensive method for measuring instantaneous velocity at one point in a two-dimensional (2D) fluid. The performance of the technique is comparable to that of the commercial devices, such as HWA and LDV. The working principle of our device is based on the fact that when a beam is deflected by a small external force $\mathbf{f}_{\text{ext}}$, its displacement $\delta\mathbf{r}$ is proportional to $\mathbf{f}_{\text{ext}}$. Moreover, if the frequency of the external excitation is less than the resonance frequency of the beam, $\delta\mathbf{r}$ and $\mathbf{f}_{\text{ext}}$ are in phase with each other. Experimentally, a high-Q harmonic oscillator is realized by a cantilever made of a single-mode optical fiber. The free end of the fiber is coupled to a flowing fluid and is tracked by a position sensitive diode array. For convenience, the device will be called an optical fiber velocimeter (OFV).

One of the main advantages of being able to fabricate velocimeters in-house and inexpensively is that it allows velocities at different spatial locations to be measured simultaneously. Such a capability is important for flow monitoring and for control in many industrial applications. It is also significant for research in fluid dynamics, especially in the study of fluid turbulence, where complex flow behavior is often quantified and characterized in terms of multipoint velocity correlation functions. Traditionally, scientists solve this problem by using the so called frozen turbulence assumption proposed by Taylor[3] some 60 years ago. According to this assumption local velocity fluctuations are simply translated by a mean flow and pass through the detection volume without significantly changing their form. The assumption thus allows spatial velocity correlation functions to be calculated from velocity time series measured by a single probe. Although Taylor's hypothesis has played a pivotal role historically in our understanding of isotropic and homogeneous turbulence, it is not universally applicable to all flows. The hypothesis fails for instance in flows that possess no mean flow (i.e., closed systems), or a mean flow not large enough compared to the turbulent fluctuations. Recent theoretical developments in turbulence also call for a need to test the so called fusion rules, i.e., asymptotes of multipoint velocity correlation functions when two or more points are collapsed into one.[4] Certain classes of rules cannot be tested using the frozen turbulence assumption with a single velocity probe.[5]

The OFV reported herein grew out of research aimed at understanding fluid flow and turbulence in two dimensions.[6] To realize the low-dimensional flow (see Sec. III for more details) we used freely suspended soap films that are forced to flow between two parallel wires under the action of gravity.[7] By way of introduction, Fig. 1 shows typical pic-

[a]Electronic mail: MKRST13@.CIS.PITT.EDU
[b]Electronic mail: XLWU@VMS.CIS.PITT.EDU

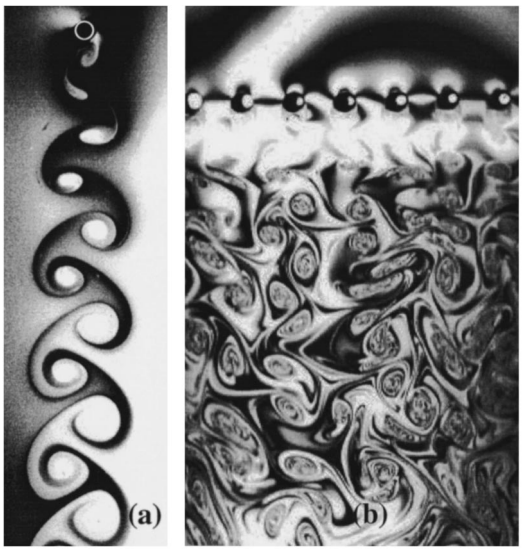

FIG. 1. Two-dimensional von Karman Street and Turbulence. A freely suspended surfactant film, bounded by two vertical wires originates about 1 m above the photographed area (see Fig. 2). At this location, the film has reached a terminal velocity of 2.5 m/s and has a nearly uniform thickness of 2 μm. Objects such as a cylindrical rod (a) and a comb or a 1D grid (b) can be inserted into the film. In the former case a von Karman street is created and in the latter 2D grid turbulence is generated. Here the rod diameter is 2 mm and the comb tooth diameter is 0.12 cm with a center-to-center distance of 0.3 cm. The pictures were taken with a 35 mm camera while the film was illuminated with a monochromatic light (a low-pressure sodium lamp). The observed flow patterns are due to film thickness variations which are coupled to the velocity field.

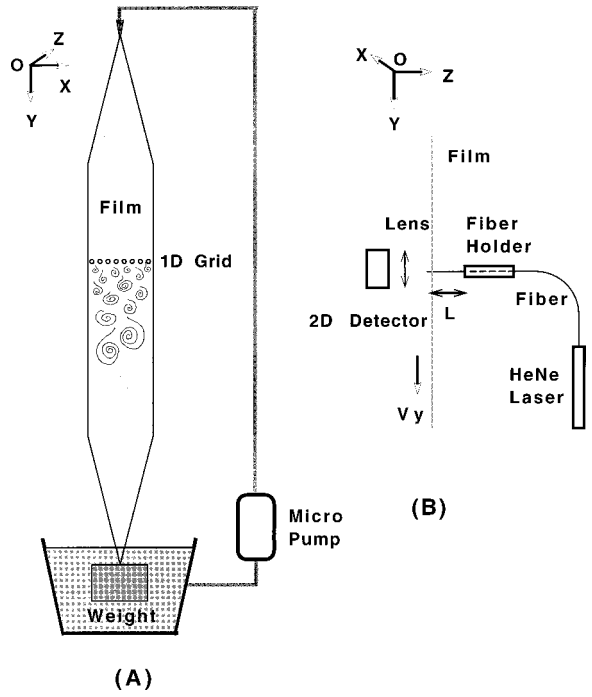

FIG. 2. (a) A schematic of the soap-film channel. The film is constantly replenished with soap solution from the top. The frame of the channel is made of nylon wires of diameter 0.08 cm. The width of the channel is 6 cm and the length is 200 cm. (b) A schematic of the OFV setup. The fiber penetrates the film by 0.5 mm. The length, measured from the fiber holder to the tip, is 5 mm.

tures taken using an interferometric technique. The spatial light intensity modulations are a result of thickness variations which behave quantitatively as a passive tracer[8] and thus provide a convenient means of flow visualization in flowing soap films. In these pictures the mean velocity, which is about 2 m/s, points downward. The velocity disturbances are caused by inserting a cylindrical rod (a) or a comb (b) into the flow. In the former case a familiar von Karman street is created, whereas in the latter case, strong interactions between vortices make the flow turbulent. Because of small film thickness, which is on the order of a few microns, the velocity variation is insignificant inside the film and the predominant velocity fluctuations $\mathbf{v}(x,y)$ are in the plane of the film and are thus 2D. The OFV was tested against a two-channel LDV for both type of flows as displayed in Fig. 1. Good agreement between the two techniques was found. Although the OFV has been used primarily in freely suspended soap films, we believe that it is applicable to a variety of flows that are strongly 2D. Interesting examples include turbulent boundary layers,[9] liquid curtains,[10] hydraulic jump,[11] and flow of shallow fluid layers on solid surfaces,[12–14] to name just a few.

This article is organized as follows. In Sec. II, we describe the experimental setup, which includes the operation of the 2D soap-film channel, the implementation of the OFV, and data acquisition. Section III contains a linear response analysis of a cantilever that is viscously coupled to a flowing film. Measurements carried out using the OFV and the LDV are presented in Sec. IV. And finally in Sec. V we discuss limitations as well as potential applications of the OFV.

II. EXPERIMENT

A. Two-dimensional soap film channel

The OFV was tested in a flowing soap-film channel that was originally designed for studying 2D turbulence.[6,15] In the following we provide a brief description of the channel. Interested readers should see Ref. 7 for more details. The channel is constructed by suspending two nylon wires from a plastic nozzle as shown in Fig. 2. The wires are held taut by a weight immersed in a soap reservoir and kept parallel with a distance ranging from 0 to 10 cm. The soap solution used for the experiment contains 1% liquid detergent (Dawn by Proctor and Gamble Co.) and 99% of water. A metered amount of soap solution is injected at the top of the channel and collected and recycled at the base. Depending on the injection rate, the mean speed of the film can be varied between 0.5 and 4 m/s. Continuous feeding of the soap solution makes the film very robust, so that it lasts almost indefinitely.

Objects placed in the film create velocity fluctuations downstream, such as those shown in Fig. 1. The velocity can be periodic in time [Fig. 1(a)] when a rod is inserted, or spatiotemporally chaotic or turbulent [Fig. 1(b)] when a grid is inserted. We caution however that the striations in the pictures are not the velocity field, directly but rather striations in the thickness field $h(x,y)$ that are nearly passively convected by the velocity.[8] Experimentally, we found that the fractional variation of film thickness $\delta h/h$ is about 5% in laminar flow and increases 10%–20% in turbulent flow. The thickness modulations can be readily observed by illuminating the film with monochromatic light, and thus provide a

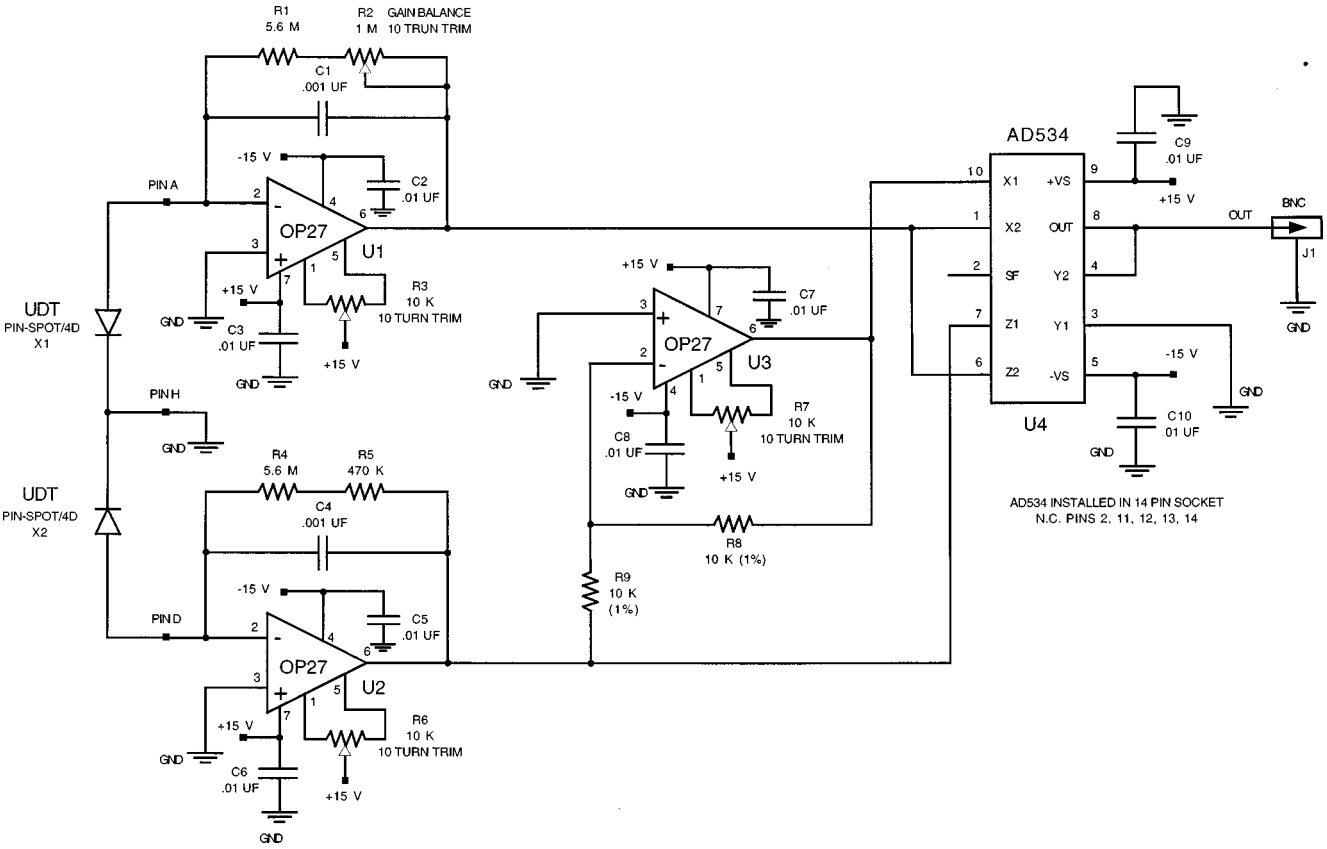

FIG. 3. Circuit diagram.

convenient, instantaneous global flow visualization. It is the flow types suggested by the images in Fig. 1 that the OFV is meant to measure.

B. OFV setup

Our OFV is made of a single-mode optical fiber with one end of it etched down to a diameter of 50 μm. The etching is carried out at room temperature (25 °C) using hydrofluoric acid (48%). A proper timing (typically 15–30 min) allows fiber tips with different diameters to be made. The etched fiber is snugly fixed into the bore of a syringe needle and fixed in place by wax. The protruding part of the fiber (with length L) acts as a cantilever with a resonance frequency determined by the Young modulus, the diameter and the length L of the fiber, as will be shown in Sec. III. For $L \simeq 0.5$ cm, f_0 is a few kHz. For the measurements, the tip of the fiber is thrust through a flowing soap film while the other end is coupled to a 5 mW HeNe laser via an optical coupler. The laser beam transmitted through the (etched) fiber tip is approximately Gaussian and is projected onto a 2D positional sensitive diode (PSD) array (United Detector Tech. Inc., PIN-Spot/4D) using a $\times 20$ microscope objective lens. The optical magnification is about ten. To reduce the environmental noise the entire setup is mounted on a vibration isolated optical table.

C. Electronics

The electronic circuit for converting signals from PSD to the displacement of the fiber tip can be constructed using off-the-shelf components. Figure 3 shows one of the two channels of the OFV. The input ends of the diodes are two identical transimpedance amplifiers. The output from the voltage divider (AD534) performs the following operation: $V_{\text{out}}=(V_a-V_b)/(V_a+V_b)$, where V_a and V_b are proportional to the photocurrent from diodes a and b. Within the proper range of the input voltage, V_{out} is proportional to the displacement of the laser beam from the center of the diode array. Experimentally we found that the output voltage from either the x or the y channel is linearly proportional to the displacement of the fiber with a sensitivity of ~ 40 mV/μm. The small voltage signal is further amplified and filtered ($0 < \Delta f < 10$ kHz) by a low-noise amplifier (EG&G 130) before it is digitized by a PC card (National Instrument AT-MIO 16XE50) with a 16-bit resolution.

III. THEORY OF OPERATION

The basic idea behind the OFV is a simple one: a simple harmonic oscillator inserted into a flow will be displaced from its equilibrium position due to hydrodynamic drag. If the oscillator is sufficiently small and operates in the linear regime, the drag force will be linearly proportional to the local velocity of the fluid. Therefore by tracking the motion of the oscillator in a fluid, one should be able to extract velocity information from the flow. What follows is a discussion of how the OFV may be considered as a subresonant simple-harmonic oscillator and be used to measure velocity in a flowing soap film.

The fiber is modeled as a uniform beam with length L, cross-sectional area πR^2, and mass density ρ.[16] To simplify the calculation the motion is assumed to be 1D. The differential equation describing the motion of a circular beam can be derived using continuum mechanics with the result:[16]

$$\frac{\partial^2 s}{\partial t^2}+\gamma\frac{\partial s}{\partial t}+c^2\frac{\partial^4 s}{\partial x^4}=\frac{F(t,x)}{\mu}, \tag{1}$$

where $s(x)$ is the displacement of the fiber from its equilibrium position, x is the distance measured from the base where the fiber is held fixed, γ is the air damping coefficient which has a dimension of inverse time, $F(x,t)$ is the external force per unit length, and $\mu=\pi R^2\rho$ is the mass per unit length. The constant c in Eq. (1) is defined as $c=\sqrt{EI/\mu}$ with E being the Young modulus and $I=\pi R^4/4$ the moment of inertia of the *section* about a line through the centroid in the plane of bending.[16]

Hydrodynamic drag on a cylinder has been studied extensively, and it is known that the drag force depends on the Reynolds number $\mathrm{Re}\equiv 2R\Delta v/\nu$, where R is the radius of the cylinder, Δv is the relative velocity between the cylinder and the background flow, and ν is the kinematic viscosity.[9] In our case Δv is defined as $\Delta v=v-(\partial s(L)/\partial t)$ with v being the flow velocity in the film and $\partial s(L)/\partial t$ the tip velocity of the fiber. The drag force (per length) in general can be written as:

$$F(x,t)=\frac{1}{2}C_D(\mathrm{Re})\rho R^2\left(v-\frac{\partial s(x)}{\partial t}\right)^2\left(\frac{h}{L}\right)\delta(x-L), \tag{2}$$

where h is the film thickness, ρ is the density of the fluid, $C_D(\mathrm{Re})$ is the drag coefficient, and the delta function $\delta(x-L)$ ensures that the force acts on the tip of the fiber. For small Reynolds numbers ($\mathrm{Re}<4$), $C_D(\mathrm{Re})\simeq 12\pi/\mathrm{Re}$, and one finds $F\propto 6\pi\eta R\Delta v$, which is the Stokes drag force. For very large Reynolds numbers ($\mathrm{Re}>1000$), $C_D(\mathrm{Re})$ is independent of Re and one recovers the well-known result of turbulent drag with $F\propto\frac{1}{2}\rho R^2\Delta v^2$.[9] For our experiment, Re is around 10^2 and to a good approximation $C_D(\mathrm{Re})\propto 1/\mathrm{Re}^{\alpha}$ ($\alpha\simeq 0.3$) and $F\propto\Delta v^{2-\alpha}$.[9] Equation (2) can be easily solved for flows in the Stokes regime, since in this case the forcing term is linear in Δv. For moderate to large Reynolds number flows, the equation can be solved analytically if the external forcing term can be linearized. This is the case in our experiment since the mean-flow speed $\overline{V}$ is an order of magnitude greater than the root-mean-square velocity v_{rms} in the film. Assuming $v=\overline{V}+v'$ and linearizing the force term in Eq. (2), we find

$$F(x,t)\simeq F_0+\tfrac{1}{2}c'(2-\alpha)(\nu/2R)^{\alpha}\rho R^2\overline{V}^{-1\alpha}\times\left(v'-\frac{\partial s}{\partial t}\right)\left(\frac{h}{L}\right)\delta(x-L),$$

where v' is the fluctuating part of the background flow and c' is an experimentally determinable constant. The first term in the above equation F_0 is a constant drag force due to the mean flow and is given by

$$F_0=\frac{1}{2}c'\left(\frac{\nu}{2R}\right)^{\alpha}\rho R^2\overline{V}^{2-\alpha}\left(\frac{h}{L}\right)\delta(x-L).$$

TABLE I. Physical parameters for the OFV.

Symbol	Name	Value	Units
ρ	density of quartz	2.2	g/cm^3
E	Young modulus of quartz	7.2×10^{11}	erg/cm^3
R	radius of the fiber	25	μm
L	length of the fiber	0.5	cm
η	shear viscosity of water	0.01	g/(cm/s)
ν	kinematic viscosity of water	0.01	cm/s^2
γ[a]	air damping coefficient	$\sim$0	1/s

[a]The air damping can be neglected since $\gamma\ll f_0$, where f_0 is the resonance frequency of the fiber.

Since Eq. (1) is a fourth-order equation, one needs four boundary conditions to completely specify the problem. The boundary conditions for a cantilever are:

$$s(0)=\frac{\partial s(0)}{\partial x}=0, \tag{3}$$

$$\frac{\partial^2 s(L)}{\partial x^2}=\frac{\partial^3 s(L)}{\partial x^3}=0. \tag{4}$$

Without losing generality, assume that the velocity at the tip is sinusoidal: $v'(t)=\tilde{v}\exp(i\omega t)$ with a small amplitude $\tilde{v}$. The equation of motion [Eq. (1)] can then be solved with the result:

$$s(L)=\frac{g(kL)\tilde{v}}{1+i\omega g(kL)}, \tag{5}$$

where k and ω are related by $k^4=(\omega^2-i\omega\gamma)/c^2$ and the function $g(z)$ is given by

$$g(z)=\frac{hL^2\xi}{\mu c^2}\left[\frac{\sin(z)\cosh(z)-\cos(z)\sinh(z)}{z^3[1+\cos(z)\cosh(z)]}\right], \tag{6}$$

where $\xi=6\pi\eta R$ for $\mathrm{Re}<4$ and $\xi=\frac{1}{2}c'(2-\alpha)\times(v/2R)^{\alpha}\rho R^2V^{1-\alpha}$ for $\mathrm{Re}>4$. Equation (6) has a set of resonance modes with the low-order ones occurring at $k_nL=1.875$, 4.694, 7.853, 10.996, and 14.137, corresponding to $n=1,2...5$. The higher order modes can be approximated by $k_nL\simeq(2n-1)\pi/2$. Neglecting air damping $\gamma=0$, the fundamental resonance frequency of the cantilever is given by

$$f_0=\omega_0/2\pi=\frac{0.56}{L^2}\sqrt{\frac{EI}{\mu}}=\frac{0.28R}{L^2}\sqrt{\frac{E}{\rho}}. \tag{7}$$

For the fiber used (see below), $L=0.5$ cm, $R=25$ μm, and $\rho=2.2$ g/cm^3, f_0 was found experimentally to be 1.5 kHz. This gives $E=9.0\times10^{11}$ erg/cm^3 which is comparable to the Young's modulus of quartz $E=7.20\times10^{11}$ erg/cm^3. For convenience, all the relevant parameters in the above set of equations, Eqs. (1)–(7), are listed in Table I.

A number of features of the solution in Eq. (6) deserve comment. First, we note that the high frequency modes are strongly damped, as $1/k^3$, so that the cantilever behaves essentially as a simple-harmonic oscillator. This same effect has been used for a long time in making music tuning forks. Second, we note that for an optical fiber having a large Q factor and being driven slowly, the response function of the fiber is flat over the frequency range $0<f\ll f_0$. Specifically,

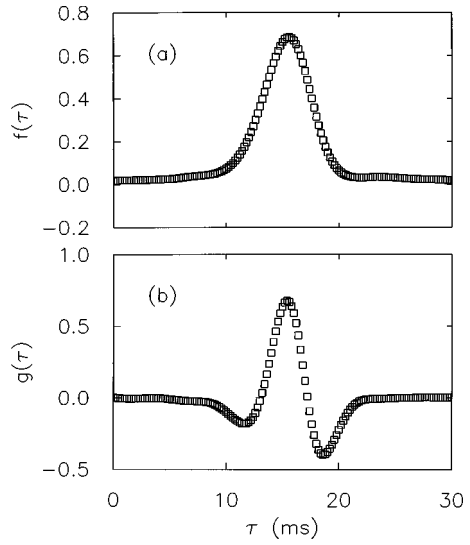

FIG. 4. Cross correlation between the OFV and the LDV: (a) the longitudinal component and (b) the transverse component. The laser beam from the two-channel LDV is focused at a point 6 cm below the grid, where 2D turbulence is generated. The OFV is placed 1.8 cm below the laser spot.

$g(x\rightarrow 0)\simeq\frac{2}{3}(h\xi L^2/c^2\mu)$, independent of f. In this regime, moreover, the tip displacement $s(L)$ is proportional to the velocity fluctuation $v'(t)$ and both quantities are in phase with each other. Characterizing the external driving force as $F_{\text{ext}}=(h/L)fv'$, the displacement at the tip of the fiber is given by

$$s(L)\simeq\frac{L^3}{E\mu}F_{\text{ext}}, \tag{8}$$

where one can define an effective spring constant $K=E\mu/L^3$ or $\pi R^4E/4L^3$. Combining Eqs. (7) and (8), we find

$$s(L)\simeq\frac{F_{\text{ext}}}{(E\rho)^{1/4}(f_0R^{5/3})^{3/2}}. \tag{9}$$

To optimize the performance of the OFV, one would like to have K as small as possible while keeping f_0 as large as possible. For a fixed frequency f_0, which can be achieved by keeping R/L^2 constant for a given material [see Eq. (7)], the sensitivity of the OFV can be greatly improved if R is reduced.

IV. MEASUREMENTS

A. Cross-correlation measurements and calibrations

A stringent test of the OFV is to directly compare velocity–time traces acquired by the OFV and LDV in the same flow. However such a measurement is difficult since the two velocity probes cannot measure velocity at the same spatial point simultaneously. A solution is to perform statistical correlations between the time traces acquired by the two probes with a finite separation. Our measurements were carried out in a soap-film channel in which flow was rendered turbulent by inserting a grid. The mean speed $V=250$ cm/s and the turbulent intensity $v_{\text{rms}}/V\simeq 15\%$. The OFV was mounted at a position 7.8 cm below the grid and a two-channel LDV (TSI Inc.) was focused at a point $l=1.8$ cm above the tip of the OFV. The LDV thus is 6 cm below the grid. The OFV used for this study has a resonance frequency of 1.5 kHz, while the LDV maintained a count rate of around 4 kHz.

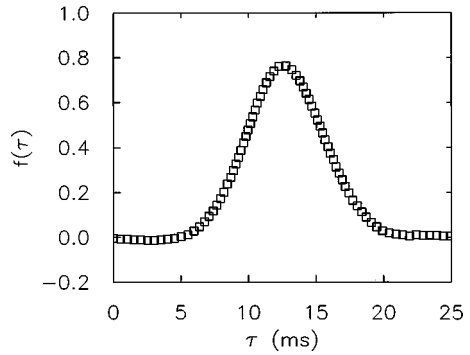

FIG. 5. The cross-correlation measurement using two LDVs. The two laser beams are separated by a vertical distance of 2 cm. The upper laser is 8 cm below the grid from which turbulence is created.

Denoting the velocity–time series measured by the OFV as $[v_x^{\text{OFV}}(t),v_y^{\text{OFV}}(t)]$ and that measured by the LDV as $[v_x^{\text{LDV}}(t),v_y^{\text{LDV}}(t)]$, the following cross correlations were calculated:

$$f(\tau)=\frac{\langle v_y^{\text{LDV}}(t)v_y^{\text{DFV}}(t+\tau)\rangle}{\sqrt{\langle v_y^{\text{LDV}}(t)^2\rangle}\sqrt{\langle v_y^{\text{OFV}}(t)^2\rangle}}, \tag{10}$$

$$g(\tau)=\frac{\langle v_x^{\text{LDV}}(t)v_x^{\text{OFV}}(t+\tau)\rangle}{\sqrt{\langle v_x^{\text{LDV}}(t)^2\rangle}\sqrt{\langle v_x^{\text{OFV}}(t)^2\rangle}}, \tag{11}$$

where v_x and v_y are the transverse and longitudinal velocity components, and $\langle\cdots\rangle$ is a time average. If the OFV measures velocity properly, then one would expect that both $f(\tau)$ and $g(\tau)$ should be peaked at a delay time $\tau_0=l/V$, as determined by the Taylor frozen turbulence assumption. This is indeed what was observed experimentally as shown in Figs. 4(a) and 4(b). For the longitudinal correlation function, $f(\tau)$ is approximately a Gaussian, whereas the transverse correlation function, $g(\tau)$ resembles that of a Mexican hat. Although the flow in our experiment is 2D, the qualitative features of both functions are rather similar to that measured in 3D fluids.[17]

We note, however, that the cross-correlation functions do not rise to one, as one would expect for identical signals, but merely to a value of 0.7. There are several reasons for this. The first and most important one is that the turbulence is still evolving during the transient time τ_0. Since $\tau_0\simeq 10$ ms is rather short, we expect that decorrelation mainly occurs for small scale velocity fluctuations. This effect is also observed even when two LDV probes configured in the same fashion are used. Figure 5 shows the longitudinal cross-correlation function [defined in Eq. (6)] measured by two LDVs that are separated by 2 cm. In this case a peak value of 0.8 was found. The somewhat higher correlation peak can be explained by the fact that in the latter measurements both LDV's were further away (by about 2 cm) from the grid. The decreased turbulence intensity downstream makes the two

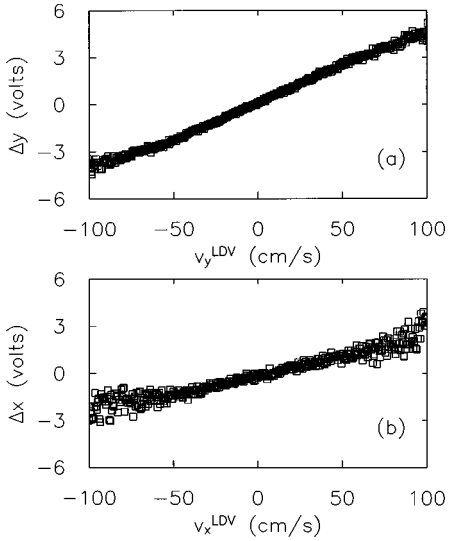

FIG. 6. Calibration curve. The horizontal axis is the velocity measured by the LDV and the vertical axis is the voltage readout from the OFV.

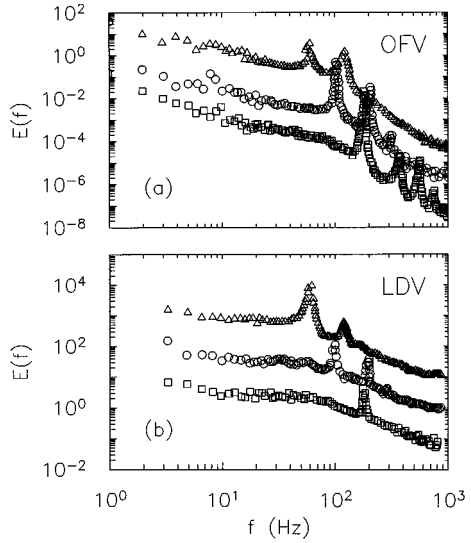

FIG. 7. Power spectra of von Karman streets measured by the OFV (a) and LDV (b). The squares, circles, and triangles are for rods with diameters 2, 4, and 7 mm, respectively. The curves are shifted vertically in the graph for a clearer viewing. We noted that as the rod diameter increases, the fundamental shedding frequency decreases. Moreover, the OFV appears to pick up high frequency component of vortex shedding more sensitively than the LDV.

LDV signals more correlated than that seen in the LDV-OFV correlation. Another source of decorrelation is the fiber's natural resonance which is readily excited in the flowing films. This mainly distorts velocity measurements in the short times (high frequency) regime.

Using the time shift τ_0 obtained from the correlation procedure we aligned the OFV and the LDV signals and averaged the OFV's output voltage for particular values of velocity as measured by the LDV. The response curve generated in this way is shown in Fig. 6. Here we have established a linear relationship between the voltage output of the OFV and the LDV readings over a surprisingly large range of velocities. This calibration procedure allows a look-up table to be generated for a given OFV and from which the OFV's output voltage can be readily converted into velocity.

B. Spectral measurements

We present a number of interesting 2D flows that have been studied using the OFV. A simple time-dependent flow in our soap film is provided by the 2D von Karman street created by a cylindrical rod as shown in Fig. 1(a). For a stable street, the velocity is periodic in time and space. If one measures a time trace at a fixed location in the wake, its Fourier transformation should consist of a set of peaks corresponding to the vortex shedding frequency. Figure 7 shows a set of measurements carried out with rods of different diameters, $D=2$, 4, and 7 mm, the mean flow being 2.3 m/s. Measurements were carried out with both the OFV (a) and the LDV (b). As can be seen in Fig. 7, the power spectra indeed exhibit sharp peaks at the fundamental frequencies of vortex shedding f^* along with high-order harmonics. The presence of the harmonics suggests that flow is not purely sinusoidal in time which is not unexpected as there are fine velocity structures within each individual vortex. Inspecting Figs. 7(a) and 7(b) we note that the OFV appears to pick up high-order harmonics more effectively than the LDV. This is presumably due to the fact that the LDV data are not sampled at even time intervals as the OFV data are. It is also observed that as the rod diameter increases the fundamental frequency f^* decreases. The effect is qualitatively the same as vortex shedding in a 3D fluid[18] although quantitatively the soap film results are quite different. For a 3D fluid, it is known empirically that vortex shedding begins at a critical Reynolds number $\mathrm{Re}_C \simeq 47$, and the shedding frequency f^* is related to the mean flow speed V and Re by the following empirical relationship: $f^* = 0.212V/D[1-(21.2/\mathrm{Re})]$.[18] In our soap films we found that this relation is not strictly obeyed and Re_C was found to be different for different diameters of rods. The conspicuously different vortex shedding behavior in 2D and 3D fluids may stem from the fact that the fluid viscosity in a soap film is a length-scale dependent quantity rather than a constant as in 3D. Our preliminary measurements suggest that as the diameter of the rods is reduced, the effective viscosity of the film decreases and approaches that of pure water with $\nu = 0.01\ \mathrm{cm}^2/\mathrm{s}$. This interesting effect is not currently well understood, and is a subject for future study.

We have also studied 2D grid turbulence in soap films using the OFV. In grid turbulence the velocity fluctuations are created at one spatial location and turbulence freely decays downstream. Freely evolving 2D turbulence has been theoretically studied by Batchelor,[17] and the energy spectrum was predicted to be $E(k) \propto k^{-3}$ for small scale fluctuations, where k is the wave number and $E(k)$ has dimensions of energy per mass per wave number. We measure $E(k)$ using a single OFV 20 cm below the grid. Longitudinal and transverse velocity time traces, $v_y(t)$ and $v_x(t)$, were accumulated over 10^6 data points and their power spectra, $\langle v_y(f)v_y^*(f)\rangle$ and $\langle v_x(f)v_x^*(f)\rangle$, were calculated. For small scales (large k), these one-dimensional spectra can be shown to be proportional to $E(k)$ if the frozen turbulence hypothesis, $k = 2\pi f/V$ is used.[19] Figure 8 shows a compari-

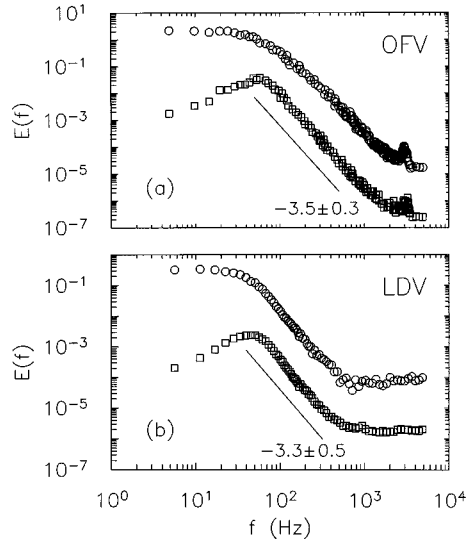

FIG. 8. Power spectra of grid turbulence. The top graph is for the OFV measurements and the lower graph is for the LDV measurements. The open circles and squares are, respectively, the longitudinal and transverse measurements. In the measurements, the mean velocity $\bar{V}$ is about 2 m/s. The same comb is used as in Fig. 1.

son between measurements using the two different techniques. Here the top graph is for the OFV and the bottom graph is for the LDV measurements. The longitudinal measurements are presented by the circles and the transverse measurements are presented by the squares. It is evident that both measurements are consistent with each other, and both reveal a k^{-3} spectrum. However the measured exponents are somewhat larger than the theoretically predicted one by about 10%. We also have found that measurements using the OFV generally yield a wider scaling range than the LDV, and the scaling exponent is also slightly larger, as shown in Fig. 8. These subtle differences are not currently well understood and shall be investigated in future experiments.

V. DISCUSSION

We have developed and tested a new device, the OFV, for measuring velocity fluctuations in a turbulent flowing soap film. Compared to the more traditional methods, such as laser Doppler velocimetry, hot-wire anemometry, and particle imaging velocimetry, the new technique enjoys a number of advantages, such as simplicity, cost effectiveness, and a fast, continuous data rate. For the velocity fluctuations that occur on the time scale slower than the inverse of the resonance frequency of the fiber, the OFV yields reliable velocity measurements.

To obtain actual velocity information it is important to calibrate each fiber with an already established technique, as we have done with a LDV. Once calibrated, the fiber may be used to extract accurate velocity information. On the other hand, if one is merely interested in statistical properties of the flow, such as power spectra which are normalized by their corresponding variances, an OFV may even be used without calibration.

Because the OFV can be readily fabricated at low cost, novel measurements are now possible. For instance one can easily measure structure function $S_n^{ij}(l)=\langle[v_i(x+l)-v_j(x)]^n\rangle$ using two fibers separated by a distance l, where i and j are the components of the velocity. For $i=j=x$, one measures the longitudinal structure function, whereas for $i=j=y$, one measures the transverse one. In order to measure $S_n^{ij}(l)$ reliably, the two fibers should be fabricated identically to ensure similar response to the flow.

In a recent development we have used two OFVs to measure circulation $\Gamma_l=\Sigma_i \mathbf{v}_i\cdot\mathbf{l}_i$ in a flowing soap film, where $\Sigma_i \mathbf{l}_i$ forms a closed square loop with sides of length l.[20] One can define a coarse-grained vorticity $\Omega_l\equiv(\Delta v_y/\Delta x-\Delta v_x/\Delta y)$, which can be shown to relate to the circulation by $\Gamma_l=\Omega_l l^2$. Here the finite differences, $\Delta v_y/\Delta x$ and $\Delta v_x/\Delta y$, are taken on the fixed scale $\Delta x=\Delta y=l$. In the experiment,[20] Ω_l was calculated using the time traces from the two probes. The first term in Ω_l is given by the finite difference between the longitudinal velocities at the two horizontal points. The second term in Ω_l is constructed using the frozen turbulence assumption: the transverse component is measured at time t and time $t+\Delta t$ such that $\bar{V}\Delta t=\Delta y=l$, where l was taken to be 1 mm. Denoting the four velocities, two for each point are recorded as (v_{x1},v_{y1}) and (v_{x2},v_{y2}), the coarse-grained vorticity is given experimentally as:

$$\Omega_l=\tfrac{1}{2}[v_{y2}(t)-v_{y1}(t)+v_{y2}(t+\Delta t)-v_{y1}(t+\Delta t)]/\Delta x - \tfrac{1}{2}[v_{x1}(t+\Delta t)-v_{x1}(t)+v_{x2}(t+\Delta t)-v_{x2}(t)]/\bar{V}\Delta t. \quad (12)$$

This method provides a simple means of measuring circulation in a flow, although it relies heavily on the Taylor's frozen turbulence assumption. In the small l limit, i.e., l being much less than the viscous dissipation scale l_d, the circulation approaches the vorticity ω at a given point in the fluid, $\Omega_l\rightarrow\omega$. To measure Ω_l independent of the Taylor hypothesis one needs at least three OFVs operating simultaneously.

ACKNOWLEDGMENTS

The authors would like to thank B. Martin and M. Rutgers for their early involvement in the project. This research is supported by the National Science Foundation and by NASA.

[1] H. H. Bruun, *Hot-Wire Anemometry, Principles and Signal Analysis* (Oxford Science, Oxford, 1995).
[2] F. Durst, A. Melling, and J. H. Whitelaw, *Principles and Practice of Laser-Doppler Anemometry*, 2nd ed. (Academic, New York, 1981).
[3] G. I. Taylor, Proc. R. Soc. London, Ser. A **151**, 421 (1935).
[4] V. L'vov and I. Procaccia, Phys. Rev. Lett. **76**, 2898 (1996).
[5] A. L. Fairhall, B. Dhruva, V. L'vov, I. Procaccia, and K. R. Sreenivasan, Phys. Rev. Lett. **79**, 3174 (1997).
[6] H. Kellay, X. L. Wu, and W. I. Goldburg, Phys. Rev. Lett. **74**, 3975 (1995).
[7] M. A. Rutgers, X. L. Wu, R. Bhagavatula, A. A. Petersen, and W. I. Goldburg, Phys. Fluids **8**, 2847 (1996).
[8] X. L. Wu, B. K. Martin, H. Kellay, and W. I. Goldburg, Phys. Rev. Lett. **75**, 236 (1995).
[9] H. Schlichting, *Boundary-Layer Theory* (McGraw–Hill, New York, 1968).
[10] S. J. Weinstein, A. Clarke, A. G. Moon, and E. A. Simister, Phys. Fluids **9**, 3637 (1997).

[11] T. Bohr, C. Ellegaard, A. E. Hansen, and A. Haaning, Physica B **228**, 1 (1996).
[12] P. L. Kapitza and S. P. Kapitza, Zh. Eksp. Teor. Fiz. **19**, 105 (1949).
[13] J. Liu and J. P. Gollub, J. Fluid Mech. **250**, 69 (1993); Phys. Fluids **6**, 1702 (1994).
[14] P. Tabeling, S. Burkhart, O. Cardoso, and H. Willaime, Phys. Rev. Lett. **67**, 3772 (1991).
[15] R. H. Kraichnan and D. Montgomery, Rep. Prog. Phys. **43**, 35 (1980).
[16] A. H. Cottrell, *The Mechanical Properties of Matter* (Wiley, New York, 1964).
[17] G. K. Batchelor, *The Theory of Homogeneous Turbulence* (Cambridge University Press, London, 1953).
[18] A. Roshko, National Advisory Committee Aeronautic Technical Notes 2913 (1953).
[19] J. O. Hinze, *Turbulence* (McGraw–Hill, New York, 1975).
[20] H. Kellay, X. L. Wu, and W. I. Goldburg, Phys. Rev. Lett. **80**, 277 (1998).